J. Membrane Biol. 158, 197–208 (1997)

The Journal of
Membrane
Biology

Facilitation of Membrane Fusion During Exocytosis and Exocytosis-Coupled Endocytosis and Acceleration of ''Ghost'' Detachment in *Paramecium* by Extracellular Calcium. A Quenched-Flow/Freeze-Fracture Analysis

H. Plattner, C. Braun, J. Hentschel
Faculty of Biology, University of Konstanz, P.B. Box 5560, D-78434 Konstanz, Germany

Received: 27 September 1996/Revised: 11 February 1997

Abstract. We had previously shown that an influx of extracellular Ca^{2+} (Ca^{2+}_e), though it occurs, is not strictly required for aminoethyldextran (AED)-triggered exocytotic membrane fusion in *Paramecium.* We now analyze, by quenched-flow/freeze-fracture, to what extent Ca^{2+}_e contributes to exocytotic and exocytosis-coupled endocytotic membrane fusion, as well as to detachment of ''ghosts'' — a process difficult to analyze by any other method or in any other system. Maximal exocytotic membrane fusion (analyzed within 80 msec) occurs readily in the presence of $[Ca^{2+}]_e \geqslant 5 \times 10^{-6}$ M, while normally a $[Ca^{2+}]_e = 0.5$ mM is in the medium. A new finding is that exocytosis and endocytosis is significantly stimulated by increasing $[Ca^{2+}]_e$ even beyond levels usually available to cells. Quenching of $[Ca^{2+}]_e$ by EGTA application to levels of resting $[Ca^{2+}]_i$ or slightly below does reduce (by ~50%) but not block AED-triggered exocytosis (again tested with 80 msec AED application). This effect can be overridden either by increasing stimulation time or by readdition of an excess of Ca^{2+}_e. Our data are compatible with the assumption that normally exocytotic membrane fusion will include a step of rapid Ca^{2+}-mobilization from subplasmalemmal pools (''alveolar sacs'') and, as a superimposed step, a Ca^{2+}-influx, since exocytotic membrane fusion can occur at $[Ca^{2+}]_e$ even slightly below resting $[Ca^{2+}]_i$. The other important conclusion is that increasing $[Ca^{2+}]_e$ facilitates exocytotic and endocytotic membrane fusion, i.e., membrane resealing. In addition, we show for the first time that increasing $[Ca^{2+}]_e$ also drives detachment of ''ghosts'' — a novel aspect not analyzed so far in any other system. According to our pilot calculations, a flush of Ca^{2+}, orders of magnitude larger than stationary values assumed to drive membrane dynamics, from internal and external sources, drives the different steps of the exo-endocytosis cycle.

Key words: Calcium — Endocytosis — Exocytosis — Membrane fusion — Secretion — *Paramecium*

Introduction

In our system, the *Paramecium* cell, we addressed the following questions. (i) To what extent does extracellular Ca^{2+} concentration, $[Ca^{2+}]_e$, affect exocytotic membrane fusion and possibly also the following steps, i.e., (ii) exocytosis-coupled endocytotic membrane resealing and (iii) detachment of empty secretory organelle membranes (''ghosts'') from the cell surface? While (i) has been thoroughly analyzed in many systems, e.g., by patch clamp analysis [2, 3, 31, 41], data on (ii) appear controversial and (iii) has not been amenable to study in any other system by any other method. In contrast, we have experimental access to all three aspects because of the particular ''design'' of our cells and of the quenched-flow methodology we developed to exploit the synchrony of our system (*see* below).

As generally accepted, exocytosis can be regulated by an increase of free intracellular Ca^{2+} concentration, $[Ca^{2+}]_i$, which may be produced by an influx of Ca^{2+}_e, by mobilization from internal pools or by both mechanisms in concert [4, 13, 14, 52, 54, 64]. In the last case, Ca^{2+} influx may precede mobilization and cause Ca^{2+}-induced Ca^{2+} release (CICR), as occurring during contraction of cardiac muscle cells [34]. Alternatively, store depletion may precede, as in skeletal muscle cells [34]. In secretory cells elements of Endoplasmic Reticulum, ER, acting as putative cortical Ca^{2+} stores may be compared with the Sarcoplasmic Reticulum, SR, in muscle cells

Correspondence to: H. Plattner

[35, 52]. In secretory cells store depletion can cause a Ca^{2+} release-activated Ca^{2+} current, CRAC, across the cell membrane [8]. For various reasons, CRAC is now thought to involve subplasmalemmal Ca^{2+} pools. This now is of considerable interest [8] although, with most systems, structural identification of such compartments is difficult. Any of these mechanisms may allow for a $[Ca^{2+}]_i$ increase upon exocytosis stimulation, from resting values between 10^{-8} and 10^{-7} M, to sub-μM, or, locally in subplasmalemmal spaces, to several 100 μM [15, 70].

The secretory system we analyze, the ciliated protozoan *Paramecium tetraurelia*, contains up to ~10^3 secretory organelles (''trichocysts'') docked at the cell membrane for immediate release. Sites of trichocyst docking and exocytosis display a clear-cut freeze-fracture appearance which is explained in Fig. 1 and the Table. Trichocyst exocytosis can be triggered, e.g., within 80 msec, by aminoethyldextran, AED [47–51] and involves mobilization of Ca^{2+} from cortical stores [16, 17, 26, 28] as well as a superimposed Ca^{2+}-influx [16, 17, 25, 26]. Trichocysts are surrounded by ''alveolar sacs,'' established Ca^{2+} stores [30, 61, 62], which cover almost all of the cell surface, except for trichocyst docking sites and ciliary bases [1]. Other established aspects are the requirement of Ca^{2+} for exocytosis, i.e., not only for exocytotic membrane fusion [16, 17, 26, 49], but also for discharge of secretory contents. In contrast to most other secretory systems, contents discharge requires $Ca^{2+}{}_e \geqslant 10^{-6}$ M [9].

Trichocyst docking sites display a clear-cut morphology, which undergoes characteristic changes (Fig. 1, Table) during synchronous AED stimulation, as shown by combined quenched-flow and freeze-fracture analysis [27, 45, 47, 48]. For instance, we can differentiate, on platinum/carbon replicas obtained from freeze-fractured cell membranes, between exocytotic and endocytotic membrane fusion and subsequent detachment of ''ghost'' (empty secretory organelle) membranes. For comparison, by patch clamping, endocytosis is difficult [56, 72] and ghost detachment after membrane resealing is impossible to analyze. Our quenched-flow equipment also allows us to vary $[Ca^{2+}]_e$ for different time periods, before and/or during stimulation. On this basis, we can now analyze the possible requirement of different steps of the exo-endocytotic cycle for $Ca^{2+}{}_e$.

We can thus ascertain for our system, by lowering $[Ca^{2+}]_e$ to 30 nM (i.e., slightly below resting $[Ca^{2+}]_i$ [26]) by EGTA chelation, that a Ca^{2+} influx is not strictly required for exocytotic membrane fusion. Despite this we can show that both, exocytotic and endocytotic membrane fusion, are accelerated by increasing $[Ca^{2+}]_e$ beyond levels a cell normally ''sees.'' Furthermore, we document for the first time that this also holds for internalization of ''ghosts,'' a novel aspect which could not be analyzed so far by any other method. Our calculations show that a vigorous flush of Ca^{2+}, partly from external and partly from internal sources (*see* ''Discussion''), occurs during an exo-endocytotic cycle and that this Ca^{2+} flush accelerates all steps of the exo-endocytotic cycle.

Materials and Methods

Paramecium tetraurelia wildtype cells, strain 7S, were grown axenically until early stationary phase and washed in 5 mM Pipes buffer pH7 with KCl and $CaCl_2$ (1 mM each) added. Cells were starved overnight and tested for exocytosis capability.

AED was used as a secretagogue [50, 51] and applied for different times in the quenched-flow apparatus described previously [27]. One volume part of cells, in the medium indicated above, was mixed with one part of aqueous 0.02% AED solution. Eventually samples were exposed to EGTA (free acid) to yield different free Ca^{2+} concentrations from 30 nM on as indicated in Results and figure captions. Resulting $[Ca^{2+}]$ values, e.g., in Figs. 2–4, 6 and 7, were calculated according to Föhr et al. [18] and controlled (within feasible concentration ranges) by a calibrated Ca^{2+}-selective electrode type ETH129 as specified in ref. [27]. Values from both methods closely coincided. According to our measurements, due to dissociation, values of $[Ca^{2+}]_e$ obtained in Ca^{2+}/EGTA mixtures (as indicated in Results and figure legends) are not remarkably affected by mixing with AED. Specifically, in experiments shown in Fig. 5 $[Ca^{2+}]_e$ was adjusted by EGTA and Ca^{2+} to different levels of actual free $[Ca^{2+}]_e$ which have been calculated and measured as indicated above. Occasionally, an excess of Ca^{2+} was added as chloride. When incubation times were varied, experiments lasting up to 2 sec were executed in the quenched-flow apparatus, while experiments over longer times were performed manually. After reducing $[Ca^{2+}]_e$ for variable times, an excess of Ca^{2+} was eventually readded with the AED solution. For details, *see* Results. Controls were run with EGTA only, i.e., during the whole time periods analyzed. In one series, cells were exposed for 90 min to 10 mM Ca^{2+} (which does not impair cells) before AED stimulation, in an attempt to load Ca^{2+} stores.

Quenched-flow included cryofixation by spraying cells into melting propane. Subsequent freeze-fracture and electron microscopic analysis was done as indicated previously [27, 45] where we have also characterized stages of the exo-endocytosis cycle (*see* Fig. 1 and the Table). In addition, fusion intermediates during endocytotic membrane fusion (as defined by [47]) have been analyzed separately in some experiments. Data sampling and evaluation was also as indicated previously [27, 45]. In Figs. 2 to 7, for better clarity, zero values are presented as small negative blocks. Statistical evaluation was by a parameter-free U-test. Significances are indicated for pairs of columns as indicated in figure legends. For instance, $P = 0.0003$ (1 *vs.* 3) in Fig. 2 indicates, that column 3 differs from column 1 with an error probability of 0.03% or by a confidence interval of >99.9%.

Results

We have first varied the time of $Ca^{2+}{}_e$ depletion by EGTA (Fig. 2). Due to rapid mixing in the quenched-flow apparatus, as indicated by efficient AED stimulation, there is no limitation by diffusion. Thus, the apparent rate of Ca^{2+} chelation by EGTA [40] during application times should allow effective binding. Indirectly, this assumption is supported by the overriding effect of prolongated AED application (Figs. 3, 4). We, therefore, attribute AED stimulation in presence of EGTA (resulting in $[Ca^{2+}]_e = 30$ nM) to mobilization of internal pools. These are probably the subplasmalemmal alveolar sacs

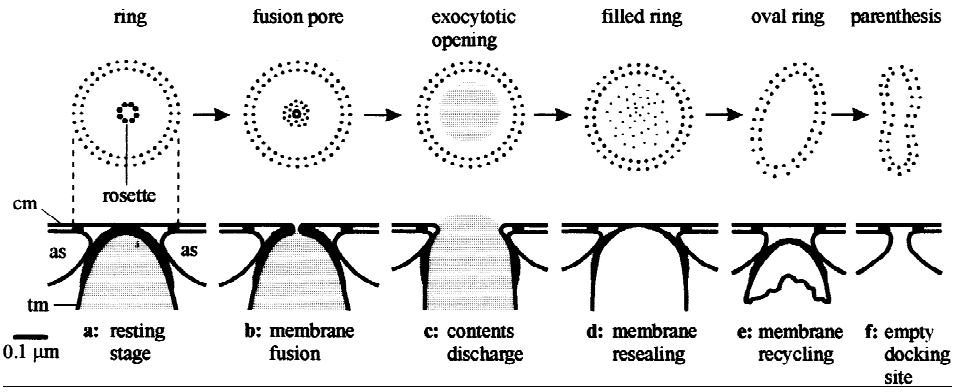

Fig. 1. Ultrastructure of trichocyst docking sites in freeze-fracture replicas (top) and in ultrathin sections (bottom). For references, *see* the Table. ''Rosettes'' formed by intramembranous particles (IMPs, integral proteins) represent sites occupied by a dischargeable trichocyst (*a*). A ''ring'' of IMPs delineates a docking/release site. Upon AED stimulation rosette IMPs decay to smaller IMPs [27] as a focal exocytotic opening is formed (*b*). This opening expands (hatched area within the ring) during trichocyst contents discharge (*c*). Resealing during endocytosis of an empty ''ghost'' results first in a ''filled ring'' (*d*, with many small loosely scattered IMPs) which collapses to an ''oval ring'' (*e*) and subsequently to a ''parenthesis'' (*f*), when the ''ghost'' is completely detached from the cell surface by internalization. Hence, a ''parenthesis'' indicates a nonoccupied potential docking site. During AED stimulation, all steps shown are accelerated by $Ca^{2+}{}_e$, as derived from the following diagrams (Figs. 2–7). Abbreviations: as = alveolar sacs (subplasmalemmal Ca-stores [28, 30, 61, 62] surrounding trichocyst docking sites), cm = cell membrane, tm = trichocyst membrane. Note coincidence of ''rings'' with rims of alveolar sacs which are closely attached to the cell membrane.

Table. Designation of exo-endocytosis stages and changes in freeze-fracture morphology of trichocyst exocytosis sites in *Paramecium*[a])

Activation stage	Freeze-fracture appearance	Stage designation
Resting	Double ''ring'' of IMPs[b]) with ~9 ''rosette'' IMPs in center	''Rosettes''
Exocytosis	''Ring'' unchanged	
Exocytotic membrane fusion	Decay of ''rosette'' IMPs to small IMPs, 10 nm fusion pore[c])	Not analyzed separately
Opening expansion	Expansion to size of ''ring''	''Openings''
Endocytosis		
Early membrane resealing	''Ring'' unchanged, 10 nm fusion pore	''Fusion intermediates''
Late stage	''Ring'' slightly collapsed to oval form with many small IMPs from ''rosette'' decay	''Filled'' or ''oval rings''
''Ghost'' detachment	Collapse of ''ring'' to ''parenthesis''-type structure	''Parentheses''

[a] Stages are as characterized by Plattner et al. [45, 47–49] and Knoll et al. [27].
[b] IMPs is equivalent to intramembranous particles or integral membrane proteins (*see* refs. [27, 49]).
[c] See ref. [27].

which could account for the quick response (*see* also ''Discussion'' for rapid cortical fluorochrome signals). We then varied $[Ca^{2+}]_e$ (Fig. 5). Finally the effect of $[Ca^{2+}]_e$ beyond usual values has been analyzed (Figs. 6, 7).

The freeze-fracture morphology allows us to identify ''resting'' exocytosis sites occupied by a dischargeable trichocyst, exocytotic openings, membrane resealing stages and unoccupied sites. For terminology, *see* Fig. 1 and the Table.

The Secretagogue Effect of AED is Reduced But Not Abolished by $Ca^{2+}{}_e$ Chelation

In Fig. 2, cells were triggered after different subsecond times of EGTA application resulting in $[Ca^{2+}]_e = 30$ nM. A reference value without EGTA incubation (−AED) shows, as a percentage of all exocytotic sites, 49% rosettes (resting stages occupied by a docked trichocyst), 0% exocytotic openings and 38% parentheses (late resealing stages or sites not occupied by a trichocyst). This indicates (i) that quenched-flow per se causes no exocytosis and (ii) that not all of the potential trichocyst docking sites are occupied. AED stimulation (−EGTA) transforms rosettes (0%) into exocytotic openings (39%). AED stimulation, after variable times of EGTA application (200–600 msec), produces less openings (8–16%) and 24–35% of rosette stages remain intact. In the whole experiment the percentage of parentheses fluctuates between 39–50% and, thus, resembles controls, with untriggered (−EGTA) or triggered (+AED) cells.

These data indicate that low $[Ca^{2+}]_e$ (30 nM) applied in the subsecond range does reduce, but cannot abolish exocytosis.

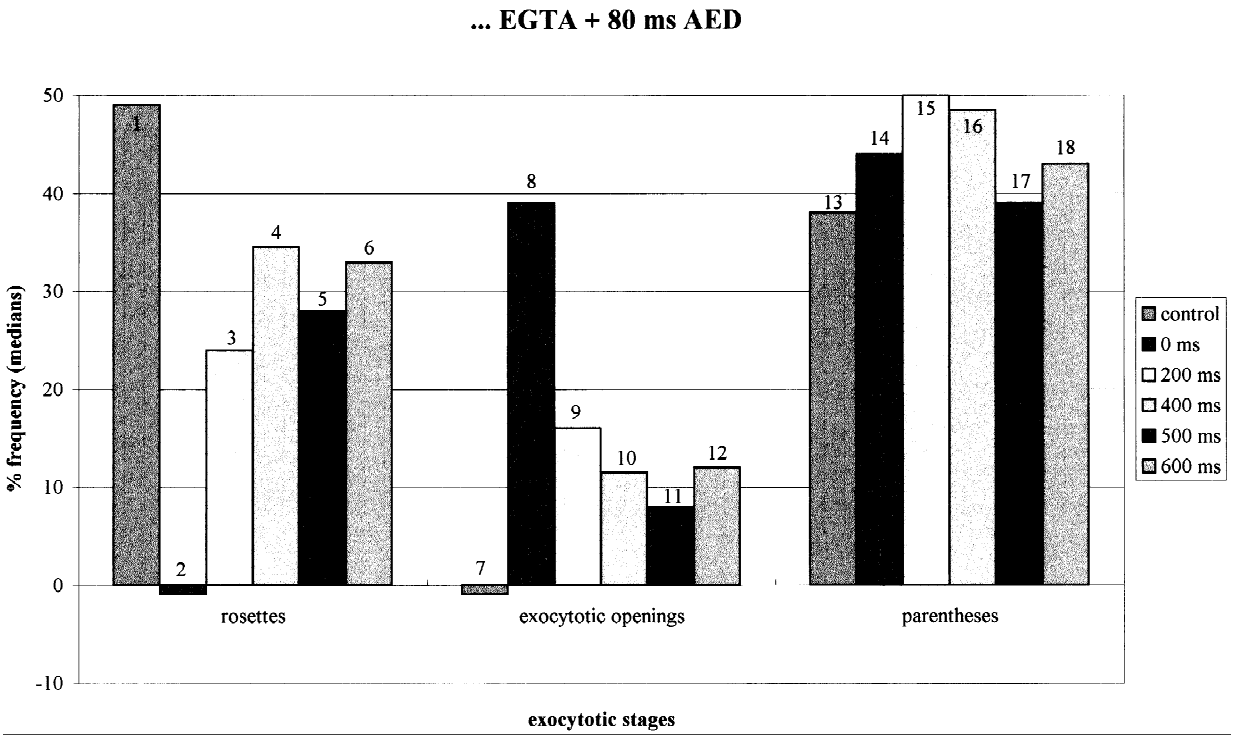

Fig. 2. Transformation of trichocyst docking sites by 80 msec AED stimulation, following different times of EGTA preincubation (resulting in $[Ca^{2+}]_e$ = 30 nM). Columns 1, 7 and 13 are for untreated controls (−EGTA, −AED). Different times of EGTA incubation in all other columns: 0 msec (control −EGTA), 200 to 600 msec EGTA incubation as indicated, before exposure to AED (for 80 msec). Data from two independent experiments. Negative columns indicate 0% values throughout figure legends. Numbers of cells (*N*) and of exocytotic sites (*n*) analyzed are indicated pairwise in this sequence for every group of columns. Statistically relevant differences (*see below*) are commented in Results. **Statistics: N,** n = 28, 429; 22, 211; 19, 303; 18, 372; 10, 144; 36, 653 for each stage. Significances (*see* Materials and Methods for details) for rosettes: $P < 0.0000$ (column 1 *vs.* column 2, designated as ''1 *vs.* 2''), 0.0003 (1 *vs.* 3), 0.04 (1 *vs.* 6), 0.04 (3 *vs.* 6); columns 1 *vs.* 4 ($P = 0.27$) and 1 *vs.* 5 ($P = 0.15$) are not or less significantly different; column 2 (0%) is significantly different from other columns ($P < 0.01$). Exocytotic openings: $P < 0.0000$ (7 *vs.* 8), 0.0002 (7 *vs.* 9), 0.001 (7 *vs.* 10), 0.06 (7 *vs.* 11), 0.001 (7 *vs.* 12); $P \leq 0.01$ for column 8 *vs.* 9 to 12; columns 9 and 12 are not significantly different ($P = 0.40$). Parentheses stages: $P = 0.08$ (13 *vs.* 15), 0.11 (13 *vs.* 18); other columns without significant difference.

Prolongated Secretagogue Application can Partially Compensate for Ca^{2+}_e Chelation

In Fig. 3 we added EGTA for 500 msec to reduce $[Ca^{2+}]_e$ to 30 nM, before we applied AED for different times (150 msec, 600 msec, 2.8 sec). In this series the control value of 49% rosettes (−AED) is slightly exceeded, for unknown reasons, by statistically nonsignificant fluctuation, by the 600 msec AED value. Untriggered controls have no exocytotic openings, while 12% occur after 150 or 600 msec AED stimulation. In controls as well as in 150 msec or 600 msec AED triggered cells, filled rings fluctuate between 0–4% and parentheses between 33–38%. Prolongation of the AED trigger to 2.8 sec reduces rosettes to 30%, no openings occur, but filled rings (9%) as well as parentheses (52%) increase significantly. Beyond confirming residual exocytotic capacity with low $[Ca^{2+}]_e$ (*c.f.* Fig. 2), the 2.8-sec values in Fig. 3 infer increased exocytotic response and increased membrane resealing (endocytosis) when the time of AED stimulation at low $[Ca^{2+}]_e$ is prolongated.

In Fig. 4 we combined different times of EGTA and/or AED application, respectively, to analyze selectively the effect on exocytotic pore formation (100% with 80 msec AED, −EGTA). Without AED, samples show no openings (no or 0.5 sec EGTA). 0.5 sec EGTA (resulting in 30 nM $[Ca^{2+}]_e$) followed by 80 msec AED results in 17% openings, i.e., ~1/5 of that in maximally triggered controls. This value is close to that in Fig. 2. When EGTA incubation was extended to 20 sec, AED stimulation time also had to be extended to achieve any significant formation of exocytotic openings. Only with $\geqslant$1 sec AED, openings increase, most significantly in this series, e.g., when AED was applied for 15 sec (after 20 sec EGTA). However, incubation with EGTA alone ($[Ca^{2+}]_e$ = 30 nM) beyond 20 sec might also provoke side effects (*see* 35-sec application of EGTA only), while Figs. 5 and 6 (below) show no significant artifactual

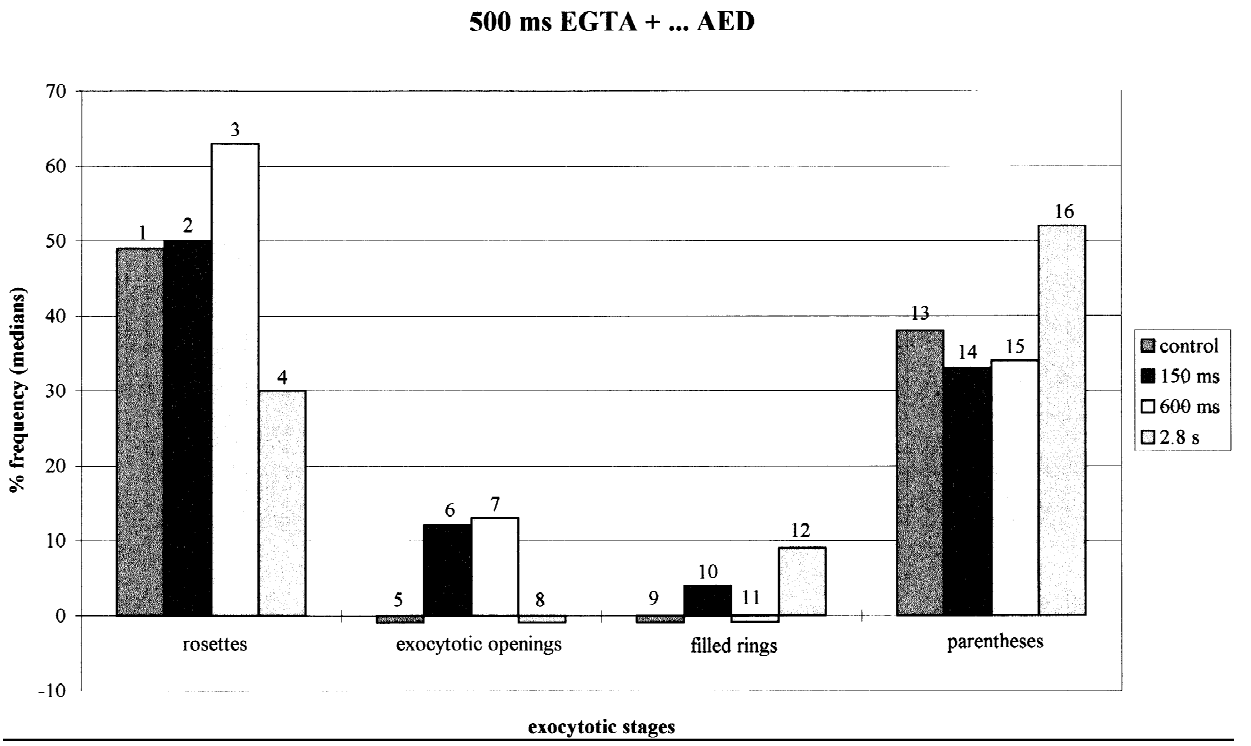

Fig. 3. Transformation of docking sites after 500 msec EGTA preincubation resulting in $[Ca^{2+}]_e$ = 30 nM, followed by different times of AED stimulation (150 msec, 600 msec, 2.8 sec). Control: 500 msec EGTA only, no AED. **Statistics: N,** *n* (as indicated in Fig. 2): 28, 428; 11, 242; 15, 464; 21, 609. Significances for rosettes: $P = 0.003$ (1 *vs.* 4); no significant difference between other columns. Exocytotic openings: $P = 0.04$ (5 *vs.* 6), 0.004 (5 *vs.* 7), 0.16 (6 *vs.* 8), 0.02 (7 *vs.* 8); columns 5, 8 and 6, 7 are not significantly different. Filled rings: $P = 0.05$ (9 *vs.* 12), 0.02 (10 *vs.* 12), 0.002 (11 *vs.* 12); other columns (except 0%) are not significantly different. Parentheses: $P = 0.003$ (13 *vs.* 16), 0.02 (14 *vs.* 16), 0.006 (15 *vs.* 16); no significant difference between other columns.

induction of openings by 0.5 or 20 sec-EGTA application. Similar tendencies are seen on the right of Fig. 4, i.e., not only longer AED incubation times, but also excessively prolongated (>20 sec) application of EGTA alone can produce more openings.

In extension of data from Fig. 3 those in Fig. 4 reveal that prolongated $Ca^{2+}{}_e$ deprivation can be compensated by prolongated AED stimulation. Furthermore, Fig. 4 suggests, as already stated, that the system may be affected when $[Ca^{2+}]_e$ is kept below resting $[Ca^{2+}]_i$ for more than 20 sec.

Increasing $[Ca^{2+}]_e$ Accelerates Exocytotic and Endocytotic Membrane Fusion

What is the response to AED (80 msec) when $[Ca^{2+}]_e$ is reduced for 20 sec to different levels, i.e., from normal values (0.5 mM) to below resting $[Ca^{2+}]_i$ values? This is analyzed in Fig. 5. Controls (−EGTA, −AED) display 73% of sites occupied by rosettes and none by openings or filled rings (resealing stages). The rest would be parentheses which are not listed separately, in this case. Even with 20 sec incubation at the lowest $[Ca^{2+}]_e$ values tested, 80 msec AED causes some decrease of rosettes and some formation of openings, while filled rings are not formed. With $[Ca^{2+}]_e \geqslant 5 \times 10^{-6}$ M, the number of openings raises considerably. These are increasingly transformed to filled rings as $[Ca^{2+}]_e$ is increased.

These data show that exocytotic openings are resealed by transformation into the stage which we call ''oval'' or ''filled rings'' (= early resealing stages). This transformation, directly or indirectly, depends on $[Ca^{2+}]_e$ (*see* Discussion).

Exocytotic and Endocytotic Membrane Fusion As Well as Ghost Retrieval Are Accelerated by Unusually High $[Ca^{2+}]_e$

What is the effect of $Ca^{2+}{}_e$ deprivation ($[Ca^{2+}]_e$ = 30 nM for 500 msec) on AED response (600 msec), when cells are preincubated for 90 min with 10 mM Ca^{2+} or when an excess of Ca^{2+} (2 mM) is supplied during AED stimulation? We show in Fig. 6 that preloading cells with Ca^{2+} is less efficient than increasing $[Ca^{2+}]_e$ to unusually high levels during stimulation. (Usually cells live in media with ~10^{-4} M Ca^{2+}, though they tolerate 10 mM without

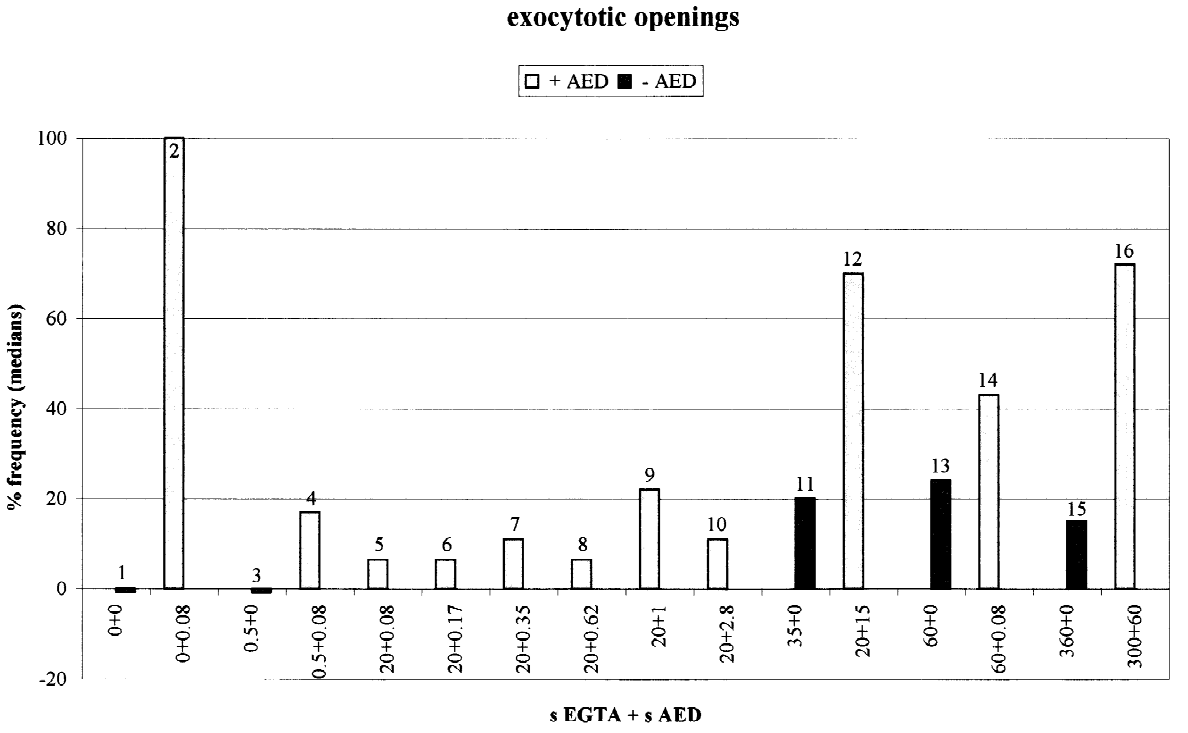

Fig. 4. Formation of exocytotic openings after different combinations of EGTA (resulting in $[Ca^{2+}]_e$ = 30 nM) and AED application for different time periods, as indicated at the bottom of the figure (e.g., ''0 + 0'' designates controls not exposed to EGTA and not stimulated by AED, ''0.5 + 0.08'' designates samples exposed for 0.5 sec to EGTA and for 0.08 sec to AED). Note that dark columns were obtained without AED application. Negative controls (−EGTA, −AED) contained no exocytotic openings (first column), while positive controls (maximally stimulated by AED without EGTA application, second column) displayed 62% of all sites analyzed with openings (normalized to 100%). Other columns (3–16) obtained after 0.5 to 360 s EGTA application and up to 60 s AED application are commented in Results. Data from 2 to 3 independent experiments. **Statistics: N,** *n* (as in Fig. 2): 65, 1669; 27, 316; 13, 197; 10, 144; 58, 1184; 27, 669; 51, 1354; 37, 1081; 23, 570; 30, 969; 47, 939; 31, 708; 12, 264; 10, 273; 10, 252; 3, 27. Significances for columns 1 to 16: $P = 0.0000$ (1 *vs.* 2), 0.15 (3 *vs.* 4), 0.004 (9 *vs.* 12), 0.0000 (11 *vs.* 12), 0.06 (13 *vs.* 14). For columns 15 and 16, too few data are available to ascertain statistical significance. No significant differences ascertained between other columns (0% values *vs.* other values not tested separately).

reacting by exocytosis). Figure 6 contains two controls with 500 msec EGTA, followed by 600 msec AED or again by EGTA, respectively. The number of sites occupied by rosettes is 63 or 67%, respectively, neither openings nor filled rings occur, and 34 or 27% of sites, respectively, are parentheses. These control values are well within the range of other experiments shown. Preincubation with Ca^{2+}, followed by AED stimulation, causes some reduction of rosettes (by ~1/3), formation of some exocytotic openings (13%) and formation of some filled rings (10%), while parentheses remain unchanged. Readdition of Ca^{2+} (2 mM) during AED triggering reduces rosettes to ~1/4 of controls. Under these conditions, no exocytotic openings are recognized, most probably because of rapid transformation into filled rings (28%) and to parentheses. Surprisingly these increase by ~2/3 as compared to controls. From Fig. 6 we conclude that preloading cells with Ca^{2+} can only in part compensate for Ca^{2+} deprivation. Compensation with higher efficiency is achieved by increasing $[Ca^{2+}]_e$ during stimulation. Figure 6 also implies that 20-sec Ca^{2+} deprivation, as used in Figs. 4 and 5, has no latent deleterious effects.

In both Figs. 5 and 6, resealing is accelerated with increasing $[Ca^{2+}]_e$. In addition, Fig. 6 not only indicates increased endocytotic membrane resealing (indicated by increased numbers of filled rings), but the increased number of parentheses also indicates the stimulating effect of increased $[Ca^{2+}]_e$ on detachment of ghosts.

As shown in Fig. 6, increased $[Ca^{2+}]_e$ activates different stages of exo- and endocytosis. This aspect was analyzed in more detail in Fig. 7. Different times of EGTA application, resulting in $[Ca^{2+}]_e$ = 30 nM, were eventually combined with different amounts of Ca^{2+} added to AED and with different times of AED application. Furthermore, ''fusion intermediates'' during membrane resealing, showing ~10 nm focal fusion stages first presented in ref. [47], were registered separately.

In this series, controls ($[Ca^{2+}]_e$ = 30 nM) without AED revealed 57% of sites with rosettes and 34% with parentheses, but no other stages. Positive controls with 80 msec AED had only 2% rosettes, but 56% openings.

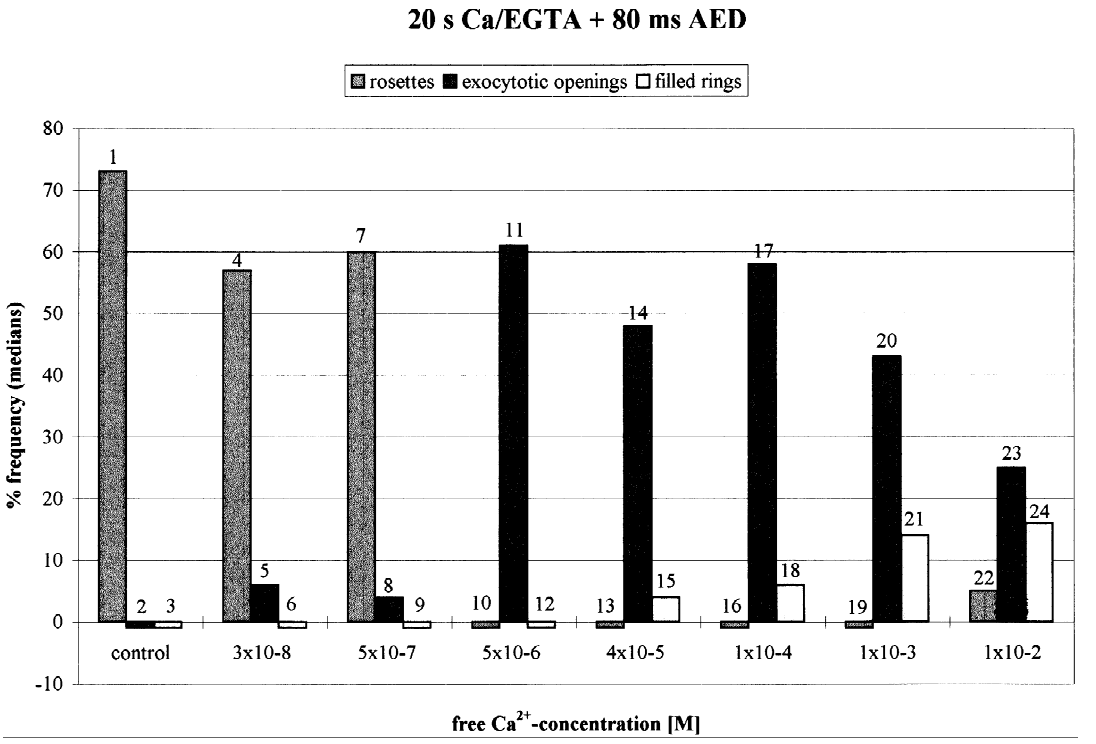

Fig. 5. Transformation of docking sites after 20 sec EGTA application resulting in the increasing free $[Ca^{2+}]_e$ values indicated below, followed by 80 msec AED application. Data from 3 independent experiments. Note increased formation of exocytotic openings from $[Ca^{2+}]_e = 5 \times 10^{-6}$ M on, as well as increased formation of resealing stages (''filled rings'') as $[Ca^{2+}]_e$ is further increased. **Statistics: N,** *n* (as in Fig. 2): 28, 460; 24, 483; 29, 443; 25, 394; 30, 548; 44, 806; 29, 410; 32, 636. Significances relevant for interpretation of columns 1 to 24: $P = 0.13$ (1 *vs.* 4), 0.03 (1 *vs.* 7), 0.09 (2 *vs.* 5), 0.16 (2 *vs.* 8), 0.0000 (8 *vs.* 11), 0.015 (12 *vs.* 15), 0.0001 (12 *vs.* 18), 0.0000 (12 *vs.* 21), 0.0000 (12 *vs.* 24), 0.09 (18 *vs.* 24). Significance of 0% values *vs.* other values was not analyzed separately.

In both of these controls, the number of parentheses varied between 21 and 34%. While interestingly no fusion intermediates occurred, AED produced 13% filled rings. The third columns were achieved with 80 msec AED with 5.5 mM Ca^{2+} added. This clearly caused rapid transformation of openings to fusion intermediates, filled rings and parentheses. These tendencies also could be verified, under similar conditions but with prolongated EGTA incubation, in columns 4 to 6 of Fig. 7. In detail, AED, in presence of EGTA, produced some openings, but no fusion intermediates or filled rings. Under similar conditions, but with $[Ca^{2+}]_e = 0.5$ mM, some openings were induced, as were some intermediates and many filled rings. When $[Ca^{2+}]_e$ was further increased to 2 mM, again subsequent to 20 sec EGTA application, the number of persisting rosettes decreased, surprisingly few openings occurred, while later stages increased considerably. In detail, intermediates increased to 6%, filled rings to 25% and parentheses to 48%.

These findings again clearly indicate that elevation of $[Ca^{2+}]_e$ favored a series of events, i.e., exocytosis, membrane resealing via fusion intermediates, transformation to filled rings and their collapse to parentheses. The latter step indicates increased detachment of trichocyst ''ghosts'' (*see* Introduction). With EGTA (500 msec) and subsequent AED (additional 600 msec) with 2 mM Ca^{2+} added (as compared to additional 600 msec EGTA, in controls), tendencies were the same as with the preceding experiments, but transformation of openings appeared even more pronounced, as this setup resulted in maximal values for filled rings and parentheses.

Discussion

Alveolar sacs resemble skeletal muscle SR by their close apposition to the cell membrane [49], their SERCA-type Ca^{2+}-pump [30, 62], their content of a calsequestrin-like protein [46] and possibly by their mode of Ca^{2+} mobilization [30, 69]. Nevertheless, the requirement of endogenous or exogenous Ca^{2+} for trichocyst exocytosis has remained controversial (*see* [17]). Therefore, we now analyzed this aspect in more detail. We try to discuss separately the possible contributions of alveolar sacs and of a Ca^{2+} influx and we also try to dissect Ca^{2+} requirements of the different steps of the exo-endocytotic cycle.

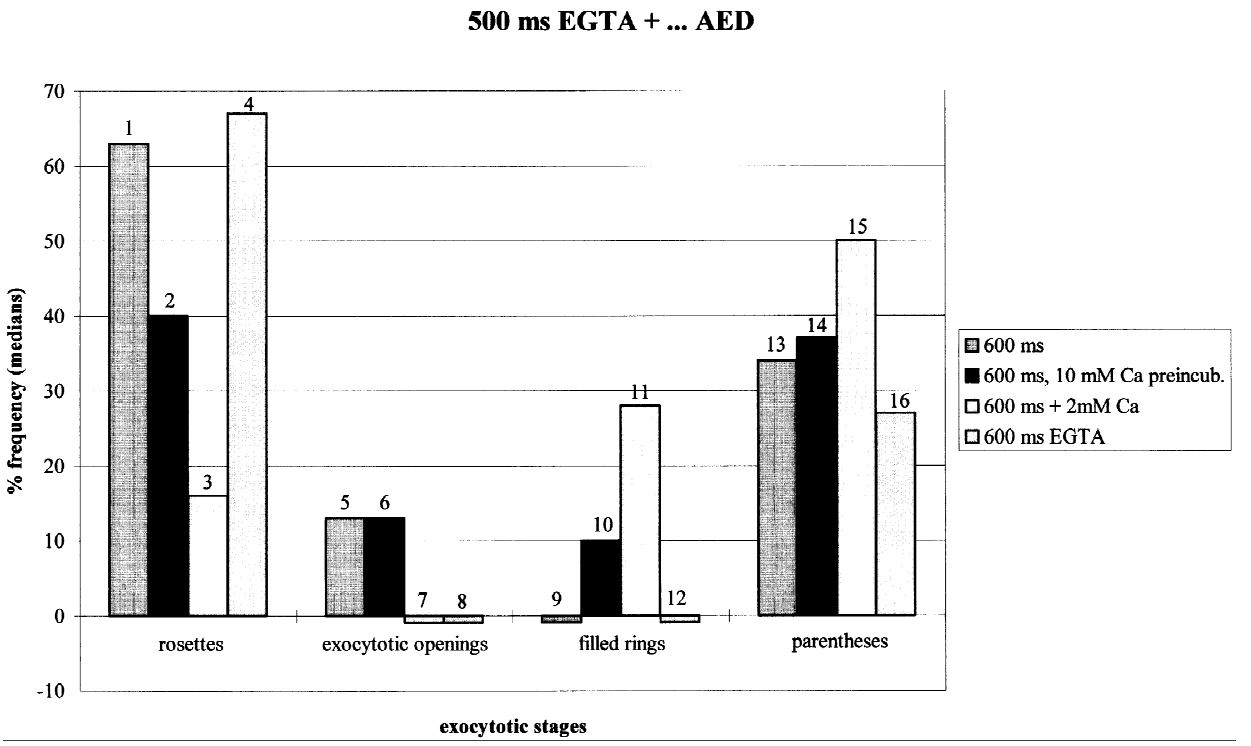

Fig. 6. Transformation of docking sites after 500 msec EGTA (to yield a basic value of $[Ca^{2+}]_e$ = 30 nM), followed by 600 msec AED with different concentrations of $[Ca^{2+}]_e$ added. First column per group: 500 msec EGTA, followed by 600 msec AED (no Ca^{2+} added) shows some exocytosis (column 5). Second column per group: the same procedure but using cells preincubated for 90 min with 10 mM Ca^{2+} (*see* Materials and Methods) results not only in some exocytotic openings but also in increased resealing stages. Third column per group: 500 msec EGTA, followed by 600 msec AED plus 2 mM Ca^{2+} added causes massive exocytosis and still more increased early and late resealing stages (''filled rings'' and ''parentheses''). Fourth column per group: 500 msec EGTA followed by 600 msec EGTA (instead of AED); this negative control shows a high percentage of ''rosettes'' (resting stages) but neither exocytotic openings nor early resealing stages (''filled rings'') and only the usual percentage of nonoccupied sites (''parentheses''). **Statistics: N,** *n* (as in Fig. 2): 15, 464; 10, 149; 20, 277; 15, 279. Significances between columns, for each of the different stages. Rosettes: $P = 0.05$ (1 *vs.* 2), 0.0000 (1 *vs.* 3); no significance between column 1 and 4 ($P = 0.24$). Exocytotic openings: $P = 0.002$ (5 *vs.* 7), 0.003 (5 *vs.* 8), 0.008 (6 *vs.* 7), 0.008 (6 *vs.* 8); no difference between columns 5 and 6. Filled rings: $P = 0.07$ (9 *vs.* 10), 0.0001 (9 *vs.* 11), 0.04 (10 *vs.* 11), 0.13 (10 *vs.* 12); no difference between column 9 and 12. Parentheses: $P = 0.05$ (13 *vs.* 15); $P \geqslant 0.3$ for other columns.

$[Ca^{2+}]_i$ in Paramecium

Based on electrophysiological data, resting values of $[Ca^{2+}]_i$ in ciliated protozoa, including *Paramecium*, have been estimated between 10^{-7} and 5×10^{-7} M [32, 33, 37–39]. In this work $[Ca^{2+}] \gtrsim 10^{-6}$ M was considered as threshold activation value because this induces ciliary reversal in permeabilized cells. Recent fluorometric evaluations showed $[Ca^{2+}]_i^{rest} = 0.5$ to 1.2×10^{-7} M, while AED stimulation resulted in a global increase to 3.5×10^{-7} M and a cortical increase to $\leqslant 10 \times 10^{-6}$ M [26]. Clearly a strong cortical Ca^{2+}-signal parallels trichocyst exocytosis within 80 msec [16] before any Ca^{2+}-signal can be registered in deeper cell layers [26]. For short times, in the ~15 nm thick interspace between cell membrane and alveolar sacs, values of several 10^{-4} M appear possible (*see* end of Discussion), as estimated also for some other exocytotic systems [57, 70, 71]. Close apposition of these Ca^{2+} stores to the cell membrane may allow for such locally high $[Ca^{2+}]_i$ which — albeit still difficult to determine — must be functionally highly important, since exocytosis rate depends on the 3rd to 4th power of $[Ca^{2+}]$ [57, 71]. Since this space is well defined, we try below to estimate any potential relevance of extra- and/or intracellular Ca^{2+} sources during AED stimulation.

Could Alveolar Sacs Potentially Provide All Ca^{2+} for Exocytosis?

Total $[Ca^{2+}]$, free and bound, in alveolar sacs has been estimated as 3 to 5 mM by secondary ion mass spectroscopic (SIMS) microscopy [61] and as 5 to 10 mM by x-ray microanalysis (XRMA, *unpublished observation* in [61]), respectively. This is well below previous XRMA

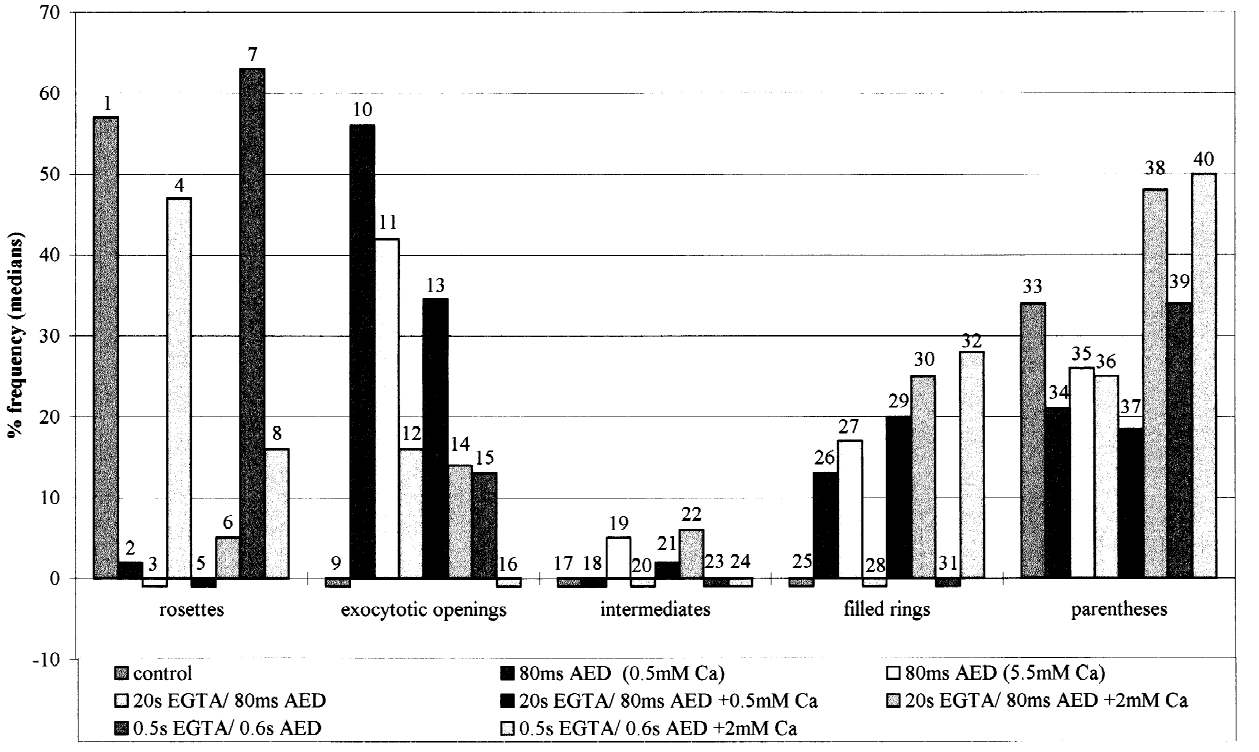

Fig. 7. Transformation of docking sites after EGTA incubation (from 0.5 to 20 sec) to yield $[Ca^{2+}]_e$ = 30 nM (unless added in excess where indicated), followed by AED application (80 msec to 0.6 sec), both over widely variable time periods. Eventually an excess of Ca^{2+} (from 0.5 to 5.5 mM) was added to the secretagogue. The sequence of experiments corresponds to horizontal reading of the legend in the bottom of the figure, i.e., from ''control'' (first in every set of columns) to ''0.5 sec EGTA/0.6 s AED + 2 mM Ca'' (last in every set of columns). Note that filled rings and particularly fusion intermediates are short-lived stages and, thus, not easily amenable to statistical analysis. For further comments, see ''Results''. **Statistics: N,** *n* (as in Fig. 2): 51, 893; 28, 659; 11, 211; 12, 245; 30, 650; 14, 295; 15, 464; 20, 277. Significance between selected columns, was tested for each of the different stages. With every stage, 0% values are significantly different from other values (not always analyzed separately). Rosettes: $P = 0.0000$ (1 *vs.* 2), 0.0007 (5 *vs.* 8); $P \geq 0.27$ for columns 1 *vs.* 4, 3 *vs.* 6, 4 *vs.* 7. Exocytotic openings: $P = 0.0000$ (9 *vs.* 10), 0.0001 (9 *vs.* 12), 0.001 (11 *vs.* 14), 0.0000 (13 *vs.* 16); no significance in (12 *vs.* 15), $P = 0.35$. Intermediates: $P = 0.007$ (21 *vs.* 24). Filled rings: $P = 0.0007$ (25 *vs.* 26). Parentheses: $P = 0.02$ (33 *vs.* 34), 0.02 (35 *vs.* 38), 0.01 (37 *vs.* 40); no significant difference between most other columns.

values of ~50 mM [58, 59], assuming 20% dry weight. Similar variation ranges were reported for SR, i.e., between 6 mM [24], 15 [23], 20 [22] and 33 mM [60], or for ER in different cells, i.e., between 1 mM [6], 1.5 to 2.5 [11], 3 [36], and 9.5 mM [7]. In sum, if one disregards excessively high values reported in older references for all of these systems, it appears reasonable to assume a total of ~5 mM Ca^{2+} in alveolar sacs.

From the SR, 40% of the stored Ca^{2+} is released per contraction cycle [24] or 59% during 1.2 sec of tetanic stimulation [60]. Similarly, with alveolar sacs, 50% were found to be released, though tested only within 30 sec (for technical reasons), during AED stimulation [61]. Since alveolar sacs on freeze-fractures appear ~10 times thicker than the subplasmalemmal space (*unpubl. observ.*), unidirectional Ca^{2+} release could yield a maximal subplasmalemmal $[Ca^{2+}]_i$ ~ 25 mM, a totally unrealistic value. This would not only reverse the concentration gradient of free Ca^{2+} in the store (*see* below), but it would also be ~10^2 fold above subplasmalemmal values occurring during stimulation in any of the secretory systems (*see* above) or in muscle cells (320 μM close to SR, [68]). This aspect will be discussed further below.

Possible Contribution of Exogenous Ca^{2+} to the Exo-Endocytosis Cycle

Similarly, one can calculate any potential subplasmalemmal $[Ca^{2+}]_i$ increase caused by Ca^{2+}-influx, based on ultrastructural details (*see above*) and on previous $^{45}Ca^{2+}$ flux measurements. AED stimulation causes a Ca^{2+} influx, culminating after ~3 sec [25], with a total uptake of 5 pM $Ca^{2+}/10^3$ cells at $[Ca^{2+}]_e$ = 0.5 mM [29]. This influx clearly exceeds the time required for exocytosis. Since ciliary membranes are not the sites of Ca^{2+} influx during AED stimulation [50], this would have to occur via the somatic membrane. Its area size is ~10.700 μm^2

[16], thus defining a subplasmalemmal space of ~161 μm^3. This would allow for an increase of $[Ca^{2+}]$ to 31 mM. This value clearly faces the same criticism as that calculated above based solely on store mobilization. We shall try to reconcile these aspects below.

Which Steps of the Exo-Endocytotic Cycle Require Ca^{2+}?

Our data show that increasing $[Ca^{2+}]_e$ accelerates completion not only of exocytosis, but also of endocytotic membrane fusion. Among a number of papers on endocytotic membrane fusion, most advocate for [5, 12, 20, 43, 53, 65, 66] and some against [55] requirement of Ca^{2+}, while some even report inhibition [19], possibly depending on the system (*see* reviews in [21, 63]). Also in Fig. 5, we show for the first time Ca^{2+} requirement for ghost detachment, as previously suggested [42]. No such data have been available for any other system.

Requirement of a Ca^{2+} Flush with Superposition from Two Sources

Our data imply a novel aspect of Ca^{2+} dynamics. The discrepancy between the actual $[Ca^{2+}]_i$ increase to be expected and the much higher values potentially produced by endogenous and/or exogenous Ca^{2+} (*see* above) may indicate requirement of a vigorous Ca^{2+} flush, rather than of stationary high $[Ca^{2+}]_i$, to drive the whole exo-endocytotic cycle. Why might such a Ca^{2+} flush be required?

Any $[Ca^{2+}]_i$ increase will be counteracted by several mechanisms. (i) Subplasmalemmal $[Ca^{2+}]$ increase will activate the Ca^{2+}-pump in the plasmalemma and in alveolar sacs [30, 62]. (ii) Some Ca^{2+} influx may occur directly into alveolar sacs [17], which thus could be replenished, in agreement with one of the models currently discussed [4]. (iii) Ca^{2+} from either source, intra- or extracellular, will be diluted by diffusion into the large cell body, as observed with fluorochromes [26]. (iv) Most Ca^{2+} will be bound to cytosolic proteins [40] and some sequestered into internal ER. Given a cell volume of 10^{-11} l, store depletion or influx would cause a global $[Ca^{2+}]_i$ increase to 0.15 or 0.5 mM, respectively. The value of free $[Ca^{2+}]_i$ as detected by fluorochromes after AED stimulation (*see* above) is again $\gtrsim 10^2$ times lower due to the activity of all of the mechanisms just discussed. Since this will also reduce cortical $[Ca^{2+}]_i$, this may explain the requirement of Ca^{2+} flush of unexpected magnitude, arising from intra- and extracellular sources in our system.

We have obtained subplasmalemmal Ca^{2+} signals of similar intensity as in alveolar sacs by electron spectroscopic imaging, 80 msec after AED stimulation [28]. We also have obtained strong, though short cortical fluorochrome signals, even with low $[Ca^{2+}]_e$, by time-resolved (33 msec) confocal laser scanning microscopy. Electrophysiology showed Ca^{2+}-activated current signals of 21 msec half-width in parallel to exocytotic events [16]. This closely resembles the Ca^{2+} increment by release from SR [67]. Under standard conditions ($[Ca^{2+}]_e = 0.5 \times 10^{-3}$ M) superposition of many such events will result in a $t_{1/2}$ of 57 or of 126 msec for exocytosis and endocytosis, respectively, for all events in all cells in our system [47].

Final Conclusions

Several assumptions on the contribution of Ca^{2+} from intra- and extracellular sources appear feasible, i.e., (i) mobilization from alveolar sacs during AED activation, followed or paralleled by (ii) a Ca^{2+} influx. Only both acting in concert can cause a strong subplasmalemmal $[Ca^{2+}]$ transient, paralleled by (iii) rapid diffusion and downregulation of subplasmalemmal $[Ca^{2+}]$. In another system, Bootman et al. [10] also recently demonstrated that, upon activation of internal Ca^{2+}-pools in HeLa cells, $[Ca^{2+}]_i$ increase strictly depends on $[Ca^{2+}]_e$, also up to 10 mM. In our cells this effect includes acceleration not only of exocytotic and endocytotic membrane fusion but, as a new aspect, also of ghost detachment by a Ca^{2+} influx superimposed to subplasmalemmal store activation. Taking into account the considerable stimulation of endocytosis by Ca^{2+}_e, Ca^{2+} could be indeed rate limiting at this step. A Ca^{2+} flush from the two sources acting in concert may serve rapid completion of the entire exo-endocytotic cycle.

This study has been supported by DFG grant P178/11 (Schwerpunkt ''Neue mikroskopische Methoden für Biologie und Medizin'').

References

1. Allen, R.D. 1988. Cytology. *In: Paramecium.* H.D. Görtz, editor. pp. 4–40. Springer-Verlag, Berlin, Heidelberg, New York
2. Almers, W. 1990. Exocytosis. *Annu. Rev. Physiol.* **52:**607–624
3. Almers, W., Neher, E. 1987. Gradual and stepwise changes in the membrane capacitance of rat peritoneal mast cells. *J. Physiol.* **386:**205–217
4. Alvarez, J., Montero, M., Garcia-Sancho, J. 1994. Agonist-induced Ca^{2+} influx in human neutrophils is not mediated by production of inositol polyphosphates but by emptying of the intracellular Ca^{2+} stores. *Biochem. Soc. Trans.* **22:**809–813
5. Artalejo, C.R., Henley, J.R., McNiven, M.A., Palfrey, H.C. 1995. Rapid endocytosis coupled to exocytosis in adrenal chromaffin cells involves Ca^{2+}, GTP and dynamin but not clathrin. *Proc. Natl. Acad. Sci. USA* **92:**8328–8332
6. Bastianutto, C., Clementi, E., Codazzi, F., Podini, P., DeGiorgi, F., Rizzuto, R., Meldolesi, J., Pozzan, T. 1995. Overexpression of calreticulin increases the Ca^{2+} capacity of rapidly exchanging Ca^{2+} stores and reveals aspects of their lumenal microenvironment and function. *J. Cell Biol.* **130:**847–855

7. Baumann, O., Walz, B., Somlyo, A.V., Somlyo, A.P. 1991. Electron probe microanalysis of calcium release and magnesium uptake by endoplasmic reticulum in bee photoreceptors. *Proc. Natl. Acad. Sci. USA* **88:**741–744
8. Berridge, M.J. 1995. Capacitative calcium entry. *Biochem. J.* **312:**1–11.
9. Bilinski, M., Plattner, H., Matt, H. 1981. Secretory protein decondensation as a distinct, Ca^{2+}-mediated event during the final steps of exocytosis in *Paramecium* cells. *J. Cell Biol.* **88:**179–188
10. Bootman, M.D., Young, K.W., Young, J.M., Moreton, R.B., Berridge, M.J. 1996. Extracellular calcium concentration controls the frequency of intracellular calcium spiking independently of inositol 1,4,5-trisphosphate production in HeLa cells. *Biochem. J.* **314:**347–354
11. Buchanan, R.A., Leapman, R.D., O'Connell, M.F., Reese, T.S., Andrews, S.B. 1993. Quantitative scanning transmission electron microscopy of ultrathin cryosections: subcellular organelles in rapidly frozen liver and cerebellar cortex. *J. Struct. Biol.* **110:**244–255
12. Burgoyne, R.D. 1995. Fast exocytosis and endocytosis triggered by depolarisation in single adrenal chromaffin cells before rapid Ca^{2+} current run-down. *Pfluegers Arch.* **430:**213–219
13. Burgoyne, R.D., Morgan, A. 1993. Regulated exocytosis. *Biochem. J. 293:*305–316
14. Cheek, T.R., Barry, V.A. 1993. Stimulus-secretion coupling in excitable cells: A central role for calcium. *J. Exp. Biol.* **184:**179–196
15. Chow, R.H., Klingauf, J., Neher, E. 1994. Time course of Ca^{2+} concentration triggering exocytosis in neuroendocrine cells. *Proc. Natl. Acad. Sci. USA* **91:**12765–12769
16. Erxleben, C., Klauke, N., Flötenmeyer, M., Blanchard, M.P., Braun, C., Plattner, H. 1997. Microdomain Ca^{2+} activation during exocytosis in *Paramecium* cells. Superposition of local subplasmalemmal calcium store activation by local Ca^{2+} influx. *J. Cell Biol.* **136:**597–607
17. Erxleben, C., Plattner, H. 1994. Ca^{2+} release from subplasmalemmal stores as a primary event during exocytosis in *Paramecium* cells. *J. Cell Biol.* **127:**935–945
18. Föhr, K.J., Warchol, W., Gratzl, M. 1993. Calculation and control of free divalent cations in solutions used for membrane fusion studies. *Meth. Enzymol.* **221:**149–157
19. Gersdorff, H.v., Matthews, G. 1994. Inhibition of endocytosis by elevated internal calcium in a synaptic terminal. *Nature* **370:**652–655
20. Heinemann, C., Chow, R.H., Neher, E., Zucker, R.S. 1994. Kinetics of the secretory response in bovine chromaffin cells following flash photolysis of caged Ca^{2+}. *Biophys. J.* **67:**2546–2557
21. Henkel, A.W., Almers, W. 1996. Fast steps in exocytosis and endocytosis studied by capacitance measurements in endocrine cells. *Curr. Op. Neurobiol.* **6:**350–357
22. Ikemoto, N., Antoniu, B., Kang, J.J., Mészáros, L.G., Ronjat, M. 1991. Intravesicular calcium transient during calcium release from sarcoplasmic reticulum. *Biochemistry* **30:**5230–5237
23. Jorgensen, A.O., Broderick, R., Somlyo, A.P., Somlyo, A.V. 1988. Two structurally distinct calcium storage sites in rat cardiac sarcoplasmic reticulum: an electron microprobe analysis study. *Circ. Res.* **63:**1060–1069
24. Kawai, M., Konishi, M. 1994. Measurement of sarcoplasmic reticulum calcium content in skinned mammalian cardiac muscle. *Cell Calcium* **16:**123–136
25. Kerboeuf, D., Cohen, J. 1990. A Ca^{2+} influx associated with exocytosis is specifically abolished in a *Paramecium* exocytotic mutant. *J. Cell Biol.* **111:**2527–2535
26. Klauke, N., Plattner, H. 1997. Imaging of Ca^{2+} transients induced in *Paramecium* cells by a polyamine secretagogue. *J. Cell Sci.* **110:**975–983
27. Knoll, G., Braun, C., Plattner, H. 1991. Quenched flow analysis of exocytosis in *Paramecium* cells: Time course, changes in membrane structure, and calcium requirements revealed after rapid mixing and rapid freezing of intact cells. *J. Cell Biol.* **113:**1295–1304
28. Knoll, G., Grässle, A., Braun, C., Probst, W., Höhne-Zell, B., Plattner H. 1993. A calcium influx is neither strictly associated with nor necessary for exocytotic membrane fusion in *Paramecium* cells. *Cell Calcium* **14:**173–183
29. Knoll, G., Kerboeuf, C., Plattner, H. 1992. A rapid calcium influx during exocytosis in *Paramecium* cells is followed by a rise in cyclic GMP within 1 s. *FEBS Lett.* **304:**265–268
30. Länge, S., Klauke, N., Plattner, H. 1995. Subplasmalemmal Ca^{2+} stores of probable relevance for exocytosis in *Paramecium.* Alveolar sacs share some but not all characteristics with sarcoplasmic reticulum. *Cell Calcium* **17:**335–344
31. Lindau, M. 1991. Time-resolved capacitance measurements: monitoring exocytosis in single cells. *Quart. Rev. Biophys.* **24:**75–101
32. Machemer, H. 1989. Cellular behaviour modulated by ions: electrophysiological implications. *J. Protozool.* **36:**463–487
33. Matsuoka, T., Watanabe, Y., Kuriu, T., Arita, T., Taneda, K., Ishida, M., Suzaki, T., Shigenaka, Y. 1991. Cell models of *Blepharisma:* Ca^{2+}-dependent modification of ciliary movement and cell elongation. *Eur. J. Protistol.* **27:**371–374
34. Meissner, G. 1994. Ryanodine receptor/Ca^{2+} release channels and their regulation by endogenous effectors. *Annu. Rev. Physiol.* **56:**485–508
35. Meldolesi, J., Villa, A. 1993. Endoplasmic reticulum and the control of Ca^{2+} homeostasis. *Subcell. Biochem.* **21:**189–207
36. Montero, M., Brini, M., Marsault, R., Alvarez, J., Sitia, R., Pozzan, T., Rizzuto, R. 1995. Monitoring dynamic changes in free Ca^{2+} concentration in the endoplasmic reticulum of intact cells. *EMBO J.* **14:**5467–5475
37. Naitoh, Y., Kaneko, H. 1972. Reactivated triton-extracted models of *Paramecium:* modification of ciliary movement by calcium ions. *Science* **176:**523–524
38. Naitoh, Y., Kaneko, H. 1973. Control of ciliary activities by adenosinetriphosphate and divalent cations in triton-extracted models of *Paramecium caudatum. J. Exp. Biol.* **58:**657–676
39. Nakaoka, Y., Tanaka, H., Oosawa, F. 1984. Ca^{2+}-dependent regulation of beat frequency of cilia in *Paramecium. J. Cell Sci.* **65:**223–231
40. Neher, N. 1986. Concentration profiles of intracellular calcium in the presence of a diffusible chelator. *Exp. Brain Res.* **14:**80–96
41. Neher, E., Marty, A. 1982. Discrete changes of cell membrane capacitance observed under conditions of enhanced secretion in bovine adrenal chromaffin cells. *Proc. Natl. Acad. Sci. USA* **79:**6712–6716
42. Pape, R., Plattner, H. 1990. Secretory organelle docking at the cell membrane of *Paramecium* cells: Dedocking and synchronized redocking of trichocysts. *Exp. Cell Res.* **191:**263–272
43. Parsons, T.D., Lenzi, D., Almers, W., Roberts, W.M. 1994. Calcium-triggered exocytosis and endocytosis in an isolated presynaptic cell: capacitance measurements in saccular hair cells. *Neuron* **13:**875–883
44. Pernberg, J., Machemer, H. 1995. Fluorometric measurement of the intracellular free Ca^{2+}-concentration in the ciliate *Didinium nasutum* using Fura-2. *Cell Calcium* **18:**484–494
45. Plattner, H., Braun, C., Klauke, N., Länge, S. 1994. Veratridine triggers exocytosis in *Paramecium* cells by activating somatic Ca channels. *J. Membrane Biol.* **142:**229–240
46. Plattner, H., Habermann, A., Kissmehl, R., Klauke, N., Majoul, I., Söling, H.D. 1997. Differential distribution of calcium stores in

Paramecium cells. Occurrence of a subplasmalemmal store with a calsequestrin-like protein. *Eur. J. Cell Biol.* **72:**297–306

47. Plattner, H., Knoll, G., Erxleben, C. 1992. The mechanics of biological membrane fusion. Merger of aspects from electron microscopy and patch-clamp analysis. *J. Cell Sci.* **103:**613–618
48. Plattner, H., Knoll, G., Pape, R. 1993. Synchronization of different steps of the secretory cycle in *Paramecium tetraurelia:* Trichocyst exocytosis, exocytosis-coupled endocytosis, and intracellular transport. *In:* Membrane Traffic in Protozoa. H. Plattner, editor. pp. 123–148 JAI Press, Greenwich, CT, London
49. Plattner, H., Lumpert, C.J., Knoll, G., Kissmehl, R., Höhne, B., Momayezi, M., Glas-Albrecht, R. 1991. Stimulus-secretion coupling in *Paramecium* cells. *Eur. J. Cell Biol.* **55:**3–16
50. Plattner, H., Matt, H., Kersken, H., Haacke, B., Stürzl, R. 1984. Synchronous exocytosis in *Paramecium* cells. I. A novel approach. *Exp. Cell Res.* **151:**6–13
51. Plattner, H., Stürzl, R., Matt, H. 1985. Synchronous exocytosis in *Paramecium* cells. IV. Polyamino compounds as potent trigger agents for repeatable trigger-redocking cycles. *Eur. J. Cell Biol.* **36:**32–37
52. Pozzan, T., Rizzuto, R., Volpe, P., Meldolesi, J. 1994. Molecular and cellular physiology of intracellular calcium stores. *Physiol. Rev.* **74:**595–636
53. Proks, P., Ashcroft, F.M. 1995. Effects of divalent cations on exocytosis and endocytosis from single mouse pancreatic β-cells. *J. Physiol.* **487:**465–477
54. Putney, J.W. 1993. Excitement about calcium signaling in inexcitable cells. *Science* **26:**676–678
55. Robinson, P.J., Liu, J.P., Powell, K.A., Fykse, E.M., Südhof, T.C. 1994. Phosphorylation of dynamin I and synaptic-vesicle recycling. *Trends Neurosci.* **17:**348–353
56. Rosenboom, H., Lindau, M. 1994. Exo-endocytosis and closing of the fission pore during endocytosis in single pituitary nerve terminals internally perfused with high calcium concentrations. *Proc. Natl. Acad. Sci. USA* **91:**5267–5271
57. Rüden, L.v., Neher, E. 1993. A Ca-dependent early step in the release of catecholamines from adrenal chromaffin cells. *Science* **262:**1061–1065
58. Schmitz, M., Meyer, R., Zierold, K. 1985. X-ray microanalysis in cryosections of natively frozen *Paramecium caudatum* with regard to ion distribution in ciliates. *Scanning Electron Microsc.* **1985-I:**433–445
59. Schmitz, M., Zierold, K. 1989. X-ray microanalysis of ion changes during fast processes of cells, as exemplified by trichocyst exocytosis of *Paramecium caudatum. In:* Electron Microscopy of Subcellular Dynamics. H. Plattner, editor. pp. 325–339. CRC Press, Boca Raton, FL
60. Somlyo, A.V., Gonzales-Serratos, H., Shuman, H., McClellan, G., Somlyo, A.P. 1981. Calcium release and ion changes in the sarcoplasmic reticulum of tetanized muscle: an electron-probe study. *J. Cell Biol.* **90:**577–594
61. Stelly, N., Halpern, S., Nicolas, G., Fragu, P., Adoutte, A. 1995. Direct visualization of a vast cortical calcium compartment in *Paramecium* by secondary ion mass spectrometry (SIMS) microscopy: possible involvement in exocytosis. *J. Cell Sci.* **108:**1895–1909
62. Stelly, N., Mauger, J.P., Kéryer, G., Claret, M., Adoutte, A. 1991. Cortical alveoli of *Paramecium:* a vast submembraneous calcium compartment. *J. Cell Biol.* **113:**103–112
63. Südhof, T.C. 1995. The synaptic vesicle cycle: a cascade of protein-protein interactions. *Nature* **375:**645–653
64. Taylor, C.W. 1994. Ca^{2+} sparks a wave of excitement. *Trends Pharmacol. Sci.* **15:**271–274
65. Thomas, P., Lee, A.K., Wong, J.G., Almers, W. 1994. A triggered mechanism retrieves membrane in seconds after Ca^{2+}-stimulated exocytosis in single pituitary cells. *J. Cell Biol.* **124:**667–675
66. Thomas, P., Surprenant, A., Almers, W. 1990. Cytosolic Ca^{2+}, exocytosis, and endocytosis in single melanotrophs of the rat pituitary. *Neuron* **5:**723–733
67. Tsugorka, A., Ríos, E., Blatter, L.A. 1995. Imaging elementary events of calcium release in skeletal muscle cells. *Science* **269:**1723–1726
68. Wendt-Gallitelli, M.F., Isenberg, G. 1989. Correlated electrostimulation and electron probe x-ray microanalysis of heart muscle cells. *In:* Electron Microscopy of Subcellular Dynamics. H. Plattner, editor. pp. 341–353. CRC Press, Boca Raton, FL
69. Zhou, X.L., Chan, C.W.M., Saimi, Y., Kung, C. 1995. Functional reconstitution of ion channels from *Paramecium* cortex into artificial liposomes. *J. Membrane Biol.* **144:**199–208
70. Zucker, R.S. 1993*a.* Calcium and transmitter release. *J. Physiologie* **887:**25–36
71. Zucker, R.S. 1993*b.* Calcium and transmitter release at nerve terminals. *Biochem. Soc. Trans.* **21:**395–401
72. Zupancic, G., Kocmur, L., Veranic, P., Grilc, S., Kordas, M., Zorec, R. 1994. The separation of exocytosis from endocytosis in rat melanotroph membrane capacitance records. *J. Physiol.* **480:**539–552